

# Modulated replica symmetry breaking schemes for antiferromagnetic spin glasses

R. Oppermann<sup>1</sup>, D. Sherrington<sup>2</sup>, M. Kiselev<sup>1</sup>

<sup>1</sup> Institute for Theoretical Physics, University of Würzburg, D-97074 Würzburg

<sup>2</sup> Department of Physics, University of Oxford, Keble Road, OX3NP UK

December 2, 2024

**Abstract.** We define modulated replica symmetry breaking (*RSB*) schemes which combine tree- and wave-like structures. A modulated scheme and unmodulated *RSB* are evaluated at 1-step level for a semiconductor model with antiferromagnetic Korenblit-Shender interaction. By comparison of the free energies we find evidence that a  $T = 0$  phase transition in the ferrimagnetic phase leads to a transition between the different *RSB*-schemes. An embedding factor of Parisi block matrices with sublattice-asymmetrical size is employed as a new variational parameter in the modulated scheme.

**PACS.** 68.35.Rh Phase transitions and critical phenomena – 75.10.Nr Spin glass and other random models

## 1 Introduction

Hierarchical tree-structures and replica symmetry breaking (*RSB*) [1, 2] are celebrated features in the theory of magnetic systems with random and frustrated interactions of infinite range. Their role for short-range spin glasses was hotly debated recently [3, 4]. A puzzling question over many years concerned the existence of variants or alternatives for the Parisi *RSB*-scheme. The latter proved to be very robust however; it is hard to find relevant variables which perturb or change the scheme.

In this article we define and apply *RSB*-schemes which show a wave-like modulation in addition to the tree-structure [1, 2]. We work in the context of a two sublattice infinite-range interaction model, defined and analyzed in replica-symmetric (*RS*)-approximation by Korenblit and Shender [5] (*KS*-model). The *KS*-model successfully offered the description of transitions between spin glass and antiferromagnetic order (or ferrimagnetic order in a field) in spite of an infinite-range interaction. Spatially staggered order is allowed by letting the interaction work only between different sublattices. The field of application includes two-component magnets as well as standard antiferromagnets, where staggered magnetic order defines sublattices. Range-free interactions cannot distinguish spatial positions and consequently unite the mean field picture of sublattice systems with another class of systems having just an equal number of mutually interacting but arbitrarily placed A- and B-spins. The *KS*-model effectively mirrors the phase diagram of the *SK*-model [6] to the antiferromagnetic side, still allowing to retrieve ferromagnetic solutions. Intra-lattice interactions are a less relevant detail [5]; they can yet be included and dealt with in a refined

*KS*-model. Transitions from spin glass to ferrimagnetic order, driven by antiferromagnetic interactions, are frequent physical phenomena and concern a wide range of different microscopic models. Even in cases when quenched disorder is weak or absent, spin glass models can have the power to mimic behaviour of clean but geometrically frustrated systems [7, 8, 9]. Beyond the present application to antiferromagnetic instabilities and ferrimagnetic glassy phases, our results suggest that the modulated *RSB*-schemes could also serve as a basis to describe excited states in finite-range spin glasses.

## 2 The two-sublattice spin glass model with competing antiferromagnetic- and ferrimagnetic order

A class of Hamiltonians, for which the modulated *RSB*-scheme is constructed, is given by the *KS*-model in an external field  $h(r)$

$$\mathcal{H} = - \sum_{i_A=1}^N \sum_{j_B=1}^N J_{i_A, j_B} S(r_{i_A}) S(r_{j_B}) + \sum_{i_A} h(r_{i_A}) S(r_{i_A}) + \sum_{i_B} h(r_{i_B}) S(r_{i_B}), \quad (1)$$

where the partially frustrated random interaction  $J_{i_A, j_B}$  is chosen to obey a Gaussian distribution  $P(J_{i_A, j_B}) = \exp(-N(J_{i_A, j_B} + J_{af}/N)^2/(2J^2))\sqrt{N/(2\pi J)}$ . Centered at a negative mean coupling  $\langle J_{i_A, j_B} \rangle = -J_{af} < 0$ , the sublattice-interaction permits glassy antiferromagnetic order.

Glassy ferrimagnetic order with lifted  $A \leftrightarrow B$  symmetry results for example when a homogeneous field is applied or when spins of different lengths (different spin quantum numbers in quantum models) happen to be located on different sublattices. Modulated *RSB* should also be considered for model classes including interactions of different types of localized spins, for example tight-binding electron spins coupled to ionic spins  $S$ ; initially mobile carriers, which localize due to their interaction with ionic spins, may not be able to fit the *RSB* glassy order. This example reaches far beyond the classical model (1). In the present work we focus exclusively on model (1) with minimal inequivalence of sites (such as being of  $A$ - and  $B$ -type), which requires a hybrid modulated form of *RSB* in a solvable classical model and hence reveals a coupling of replica- and real space.

In replica theory [10], which we use here, all spin variables acquire a replica-index  $a$ ,  $S \rightarrow S^a$ . After elimination of the microscopic spins the corresponding effective Lagrangian of the replica theory [6] is given in terms of Hubbard-Stratonovich fields [5]. The *SK*-model interaction requires one such field [6],  $\tilde{Q}^{a,b}$ . Its statistical average  $Q^{ab} \equiv \langle \tilde{Q}^{ab} \rangle = \langle S_i^a S_i^b \rangle$  describes glassy order [1,2] in addition to a homogeneous magnetization  $M = \langle S_i^a \rangle$ , which can be finite in case of partial frustration. The *KS*-model however involves for each sublattice  $\kappa = A, B$  a magnetization  $M_\kappa \equiv \langle S_{i_\kappa}^a \rangle$  and  $Q_\kappa^{ab} \equiv \langle \tilde{Q}_\kappa^{a,b} \rangle$ , and a field  $\tilde{Q}_3^{a,b}$  which couples the sublattices [5]. The averaged matrix  $Q_{AB} \equiv -i Q_3 \equiv -i \langle \tilde{Q}_3 \rangle$  turns out to be equal to  $Q_A + Q_B$ , where  $Q_A$  and  $Q_B$  inevitably show sublattice-splitting of their entries  $q_A \neq q_B$  in *ferrimagnetic* phases, together with  $|M_A| \neq |M_B|$ . The size of their block-diagonal matrices, characterized in *RSB* by a Parisi parameter  $m$  [1], may also develop a sublattice-asymmetry. Thus, at 1*RSB*-level two order parameters for each sublattice  $A$  or  $B$ , hence  $\{q_{1A}, q_{2A}, q_{1B}, q_{2B}\}$ , denoting matrix elements of  $Q_A$  and  $Q_B$ , and two Parisi-parameters  $m_A, m_B$  need to be considered. A simple illustration for  $Q_3$  is shown in Fig.1. Note that for simplicity it is not shown that elements on the diagonal vanish (or, as in fermionic spin glasses, equal 1).

*Unmodulated replica-symmetry breaking scheme:* In the unmodulated 1*RSB* scheme one chooses  $m_A = m_B$ .

### 3 Modulated Replica Symmetry Breaking Schemes

We consider the superposition of two diagonal Parisi-block matrices with sizes  $m_A \times m_A$  and  $m_B \times m_B$  such that a rational embedding factor  $\gamma$  denotes the number of smaller blocks (let  $m_A < m_B$ ) *fully embedded* inside larger  $m_B$ -boxes, i.e. without being intersected by the latter ones, divided (normalized) by the number of larger boxes inside the entire  $(n \times n)$  host matrix (the example of Fig.1 show  $\gamma = 1$  (left figure) and  $\gamma = \frac{5}{7}$  (right figure)).

We distinguish now a single embedding scheme, for which the host size  $n$  is restricted to be the least common

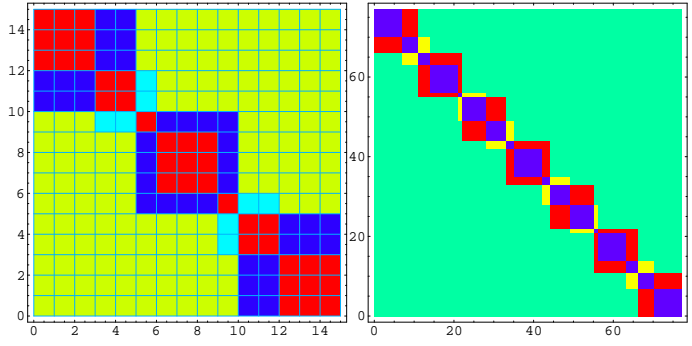


**Fig. 1.** Simple examples of modulated saddle point matrices  $Q_{AB} = Q_A + Q_B$  with  $m_A = 3$ ,  $m_B = 5$ , and  $n = 15$  (left Figure) and  $m_A = 7$ ,  $m_B = 11$ , and  $n = 77$  (right Figure) in one-step *RSB*. Four different regions are shown with entries  $q_{1A} + q_{1B}$ , generated by the overlap-areas of  $m_A \times m_A$ - and  $m_B \times m_B$ -sized block matrices along the diagonal, with  $q_{1A} + q_{2B}$  and  $q_{2A} + q_{1B}$  generated by their nonoverlap-regions, and  $q_{2A} + q_{2B}$  belonging to the superposition of off-diagonal  $A$ - and  $B$ -elements.

multiple of  $m_A$  and  $m_B$ , and multiple embedding schemes, which align  $k$ -times such structures along the diagonal. For all of  $n, m_A, m_B, n/m_A$ , and  $n/m_B$  integral and  $m_A < m_B$ , the embedding parameter  $\gamma$  is given by

$$\gamma = (n/m_A - (n/m_B - 1))/(n/m_B). \quad (2)$$

Let us now turn to the important replica limit  $n \rightarrow 0$ .

#### 3.1 Single-embedding modulated scheme (SMS)

When the limit  $n \rightarrow 0$  is approached, as required in replica theory, Eq.2 and the integral constraints associated with it must be relaxed. This allows to obtain a finite nontrivial free energy. To this end we choose  $\gamma$  as a free variational parameter like  $m_A$  and  $m_B$ . To obtain the free energy  $F$  for this modulated *RSB*-scheme we need the trace of the square of such super-imposed Parisi matrices (see Eq.6 below). The free energy involves the limit as  $n$  goes to zero of  $(1/n)$  times a sum of traces over the  $Q^2$ -values. As for standard Parisi matrices [1,2],  $\text{tr}[Q_\kappa^2] = n(m_\kappa - 1)(q_{1\kappa} + q_{1\kappa})^2 + n(n - m_\kappa)(q_{2\kappa} + q_{2\kappa})^2$ ,  $\kappa = A, B$ , so for a physical finite free energy one requires that  $\text{tr}[Q_3]^2$  also scales like  $n$  for small  $n$ . A set of self-consistent equations is derived by the condition that  $m_A, m_B$  and  $\gamma$  extremize the free energy in the replica limit. The idea is thus to find a function of  $m_A, m_B$  and  $\gamma$ , which agrees with the trace of  $Q_{AB}^2$  for integer-valued parameters allowed by the scheme, satisfies the integral constraints (2), and whose analytical continuation for small  $n$  is linear in  $n$ . This is achieved by noting that the trace formula for  $Q_3^2$  for arbitrary block-sizes  $m_A < m_B$ , which nest the host-matrix of size  $n$ , for the single-embedding scheme, is expressible in terms of  $\gamma$  as

$$\begin{aligned} \Xi(\gamma) \equiv \text{tr}Q_{AB}^2 &= n(m_A - 1)(q_{1A} + q_{1B})^2 \\ &+ n(m_B - m_A)(q_{2A} + q_{1B})^2 + n(n - m_B)(q_{2A} + q_{2B})^2 \\ &+ 2(q_{1A} - q_{2A})(q_{1B} - q_{2B})\phi(\gamma), \end{aligned} \quad (3)$$

where the dependence on the embedding factor  $\gamma$  is contained in

$$\phi(\gamma) = \frac{n}{3m_B^3} \{ (m_B - n)(m_B - (1 + \gamma)m_A) \\ [(m_B - 2n)m_B + m_A(2n(1 + \gamma) - (4 + \gamma)m_B)] \} \quad (4)$$

The result represented by Eq.(3), together with  $\phi$  given by Eq.(4), holds for all integral and non-integral (rational) values of  $\gamma$  being allowed by the construction. Let us consider a few examples, using this division into two classes with either integral or non-integral embedding factors  $\gamma$ :

i) there exists a subset of matrices, where each  $m_B$ -block hosts the same (integral) number of  $m_A$ -blocks; the left hand part of Fig.1 has given one example with  $(m_A = 3, m_B = 5, n = 15, \gamma = 1)$ . Further examples of this class are  $(2, 7, 14, 3), (4, 7, 28, 1), (3, 8, 24, 2)$ ;

ii) the right hand side of Fig.1 showed one example for the matrix-class having non-integral embedding factors with  $(m_A = 7, m_B = 11, n = 77, \gamma = 5/7)$ . Let us add a two more by  $(3, 4, 12, 2/3)$  or  $(7, 17, 119, 11/7)$ .

One can see that  $\Xi$ -contributions from all overlap regions can be expressed in terms of  $m_A, m_B, \gamma$ , while the number of these overlap regions depends explicitly on the host matrix size  $n$ .

### 3.2 Multiple-embedding modulated scheme (MMS)

We also define a modulated scheme *MMS* which incorporates a  $k$ -fold repeated *SMS*-structure (of size  $n_1 \times n_1$ ) along the diagonal of an  $n \times n$  host matrix, for example  $(4, 6, 24, 3/4)$  where  $k = 2$ . The *SMS*-matrix size is chosen as a variational parameter, kept finite while the replica limit  $n \rightarrow 0$  is taken, and finally varied to extremize  $F$ . Altogether  $m_A, m_B$ , and  $n_1$  are variational parameters, which determine the embedding factor  $\gamma(m_A, m_B, n \rightarrow n_1)$  according to Eq.(2), or  $m_A, m_B$  and  $\gamma$  are varied and their selfconsistent solutions yield  $n_1(\gamma) = m_A m_B / (m_A - m_B + m_A \gamma)$ . The free energy is obtained by means of  $\lim_{n \rightarrow 0} \Xi(n, n_1) / n$ , where

$$\Xi(n, n_1) = \Xi(\gamma(n_1))n/n_1 + n(n - n_1)(q_{2A} + q_{2B})^2 \quad (5)$$

or  $\Xi(n, \gamma) = \Xi(\gamma)n/n_1(\gamma) + n(n - n_1(\gamma))(q_{2A} + q_{2B})^2$  in case  $\gamma$  is varied. An example for a three-fold embedding is given by Fig.2. Since relation (2) is part of the definition of the *MMS* and since the replica limit maps the Parisi-type parameters  $m_A, m_B, n_1$  from  $[1, \infty]$  into the interval  $[0, 1]$ ,  $\gamma$  is thus restricted to values  $\gamma > -1$  in contrast to the *SMS*. The *MMS* also differs essentially from the *SMS* by the fact that the (A,B)-symmetric limit  $m_A = m_B \equiv m$  reduces it to the unmodulated 1*RSB*-scheme. Another possible variant of *MMS*, where the number  $k = n/n_1$  of repeated *SMS*-structures is varied, is discarded, since  $k$  cannot extremize  $F$ .

### 3.3 Upgrade of the modulated RSB-schemes

While the modulated *RSB*-schemes are initially designed for applications to glassy ferrimagnetic systems, one should

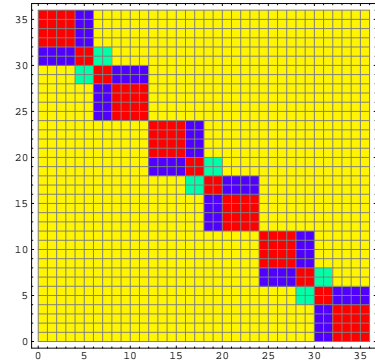


**Fig. 2.** Example of a modulated saddle point matrix belonging to the multiple-embedding scheme:  $\langle Q_3 \rangle / i = \langle Q_A \rangle + \langle Q_B \rangle$  with  $m_A = 4, m_B = 6$ , and  $n = 36$  in one-step *RSB*.

also consider them under a more general point of view: they can be used in systems without sub-lattices and even without reference to antiferro- or ferrimagnetic order. One can upgrade the schemes as an alternative of the Parisi-scheme provided the traces of higher powers  $Q^k, k \geq 3$ , also yield a non-divergent replica-limit. This separate point as well as higher order *RSB* is not the issue of the present article, where only  $\text{tr}Q_3^2$  is needed for the *KS*-model.

## 4 Application to a layer model with a confined magnetic field

In order to examine the specific features of the modulated *SMS*-scheme in comparison with the unmodulated one, we performed a detailed analysis for the *KS*-model (1) in a spatially confined magnetic field  $H_p$ . For an equal number of  $\alpha N$  of *A*- and *B*-spins we chose  $h = H_p$  and  $h = 0$  for the remaining  $(1 - \alpha)N$  spins.

The free energy of this model realization in 1-step *RSB* can be decomposed into three parts

$$F = F_0 + \alpha F_1(H_p) + (1 - \alpha)F_1(H_p = 0), \quad (6)$$

where

$$F_0 = -J_{af}M_A M_B - \frac{J^2}{4T} \left[ \lim_{n \rightarrow 0} \frac{1}{n} \text{tr}Q^2 - 2 \sum_{\kappa} (1 - q_{1\kappa}) \right], \quad (7)$$

and

$$F_1(H_p) = - \sum_{\kappa=A,B} \frac{T}{m_{\kappa}} \int_{z_{2\kappa}}^G \ln \int_{z_{1\kappa}}^G \cosh^{m_{\kappa}} \left\{ \frac{1}{T} \tilde{H}_{\kappa}(H_p) \right\} \quad (8)$$

with  $\int_z^G \equiv \int_{-\infty}^{\infty} dz e^{-z^2/2} / \sqrt{2\pi}$ , and  $\underline{Q} \equiv (Q_A, Q_B, Q_3)$ .

The effective field  $\tilde{H}_{\kappa}$  on sublattice  $\kappa$  depends on the order parameters of the complementary sublattice  $\bar{\kappa}$ . It is given in terms of 1. the confined polaron field  $H_{\kappa}$ , 2. in terms of the magnetization field of the complementary sublattice  $\bar{\kappa}$ , and 3. spin fields representing the spin glass field  $z_{k,\kappa}$  (in

the 1RSB-discretized approximation), by the expression

$$\tilde{H}_\kappa(H_p) = H_p - J_{af}M_{\bar{\kappa}} + J\sqrt{q_{2\bar{\kappa}}}z_{2\kappa} + J\sqrt{q_{1\bar{\kappa}} - q_{2\bar{\kappa}}}z_{1\kappa}, \quad (9)$$

The motivation for choosing this specification of the *KS*-model is essentially twofold:

1) by scanning the full range  $0 < \alpha < 1$  we found that the phase diagram is not only marked by a continuous spin glass - ferrimagnet transition. At slightly higher ratios  $J_{af}/J$ , a subsequent small flop transition from ferrimagnet to an (what might be called) antiferromagnetic phase occurs, which provides an ideal test-ground for the *SMS*-scheme:

the  $A \leftrightarrow B$ -symmetries are strongly broken, since solutions are far away from either  $M_A = M_B$  or  $M_A = -M_B$ . The main features of the phase diagram for all  $\alpha$  at selected characteristic polaron fields  $H_p$  and temperatures is analyzed below in 5.

2)  $CdTe/Cd_{1-x}Mn_xTe$ -layers are well described by the present model, where  $H_p$  represents a confined polaron field created by polarized exciton-hole spins being localized at the interface. The penetration depth of the hole-wavefunction defines the portion  $\alpha$  of the  $CdMnTe$ -layer which is exposed to the field  $H_p$ . The magnetic  $CdMnTe$ -layer employs Villain-Ising pseudo-spins  $S$  [11] representing tetrahedra of manganese Heisenberg-spins which retain only two orientational degrees of freedom. All pseudospins of the magnetic layer are then coupled by a long-range partially frustrated interaction with antiferromagnetic mean value. This model (with  $\alpha = 0.5$ ) provided optimal fits for experiments in the spin glass regime at  $x = 33\%$  [12]. Increasing Mn-concentration  $x$  enhances the antiferromagnetic bias and eventually leads to a transition from spin glass to antiferromagnetic or ferrimagnetic order (in a homogeneous polaron- or external field) at a critical concentration  $x_c$ . Scaling and numerical analysis on the basis of anisotropic Heisenberg models were also provided [13,14]. The virtue of the Pseudo-Ising concept lies in the smaller lower critical dimension when compared to Heisenberg systems.

We explore at  $T = 0$  the difference between the *SMS*-scheme and the unmodulated one. For its demonstration we choose a polaron-field strength  $H_p = 4J$  and a confinement-fraction  $\alpha = 0.5$  (half-penetrated layer). Our 1-step *RSB*-results are obtained by solving up to seven coupled selfconsistent integral equations (*SMS*-scheme) which extremize  $F$ . Thanks to the  $T \rightarrow 0$ -limit one integration can be solved exactly, simplifying the selfconsistent set of ten coupled double-integral equations for finite  $T$  considerably (while  $q_{1A} = q_{1B} = 1$  at  $T = 0$ , both  $q_{1\kappa}(T)$ ,  $\kappa = A, B$ , and the hole polarization too must be determined selfconsistently for finite  $T$ ). The  $T = 0$ -results of Figs.3, 4 show a continuous SG-ferrimagnetic transition with order parameter  $M_A - M_B$  to occur at  $r \equiv J_{af}/J \approx 3.25$ , followed by a discontinuous transition to antiferromagnetic order near  $r \approx 4.02$ . As Figure 3 shows,  $q_{2A}$  and  $q_{2B}$  undergo large jumps and become (almost) interchanged at the discontinuous transition in the framework of the standard unmodulated scheme, ie under the condition  $a_A = a_B$ ,  $a_\kappa \equiv \lim_{T \rightarrow 0} m_\kappa/T$ . In the modulated *SMS*-scheme, Fig.4,

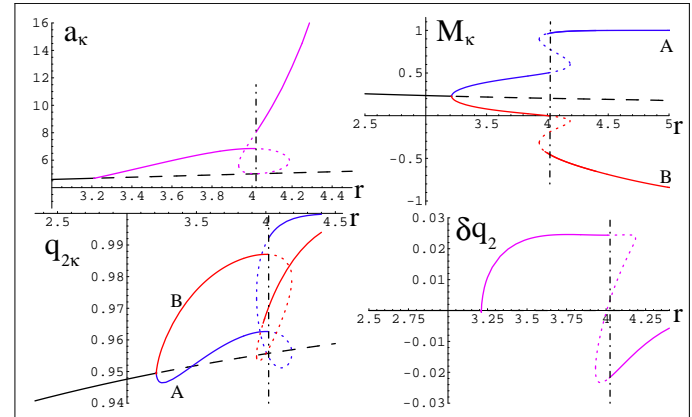


**Fig. 3.** Solutions for  $T = 0$  and  $\alpha = 0.5$  in 1-step unmodulated *RSB*: Parisi parameter  $a_A = a_B$ ,  $a_\kappa = m_\kappa/T$ , sublattice magnetizations  $M_A, M_B$ , spin glass order parameters  $q_{2A}, q_{2B}$ , and  $\delta q_2 \equiv q_{2B} - q_{2A}$ , as a function of  $r \equiv J_{af}/J$  and finite confined field  $H_p = 4J$ . Dash-dotted lines locate the 1st-order transition, dashed lines show unstable solutions.

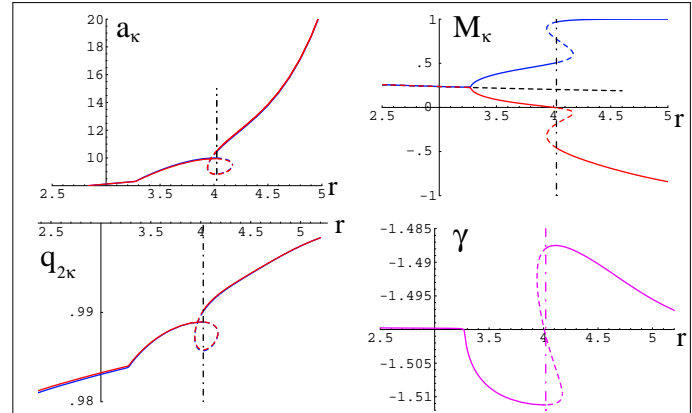


**Fig. 4.** Corresponding results in the modulated *RSB*-scheme *SMS* showing  $(a_A, a_B)$ ,  $(M_A, M_B)$ ,  $(q_{2A}, q_{2B})$ , and the *SMS*-embedding parameter  $\gamma$ . It is seen that  $a_\kappa$  and  $q_\kappa$  show only very weak sublattice splitting.

the selfconsistent solutions for  $a_A, a_B$  and  $q_{2A}, q_{2B}$  are different but show only small sublattice splitting; at the transition  $a_B - a_A$  changes sign, in contrast to  $q_B - q_A$ . The sublattice effective fields of Eq.6 help to explain the origin of the discontinuous transition: the competition between  $J_{af}M_{\bar{\kappa}}$  and the polaron field  $H_p$  leads (in the clean limit) eventually to a total spin reversal on one sublattice. Random magnetic order would smear the jump in any homogeneous field but the discontinuity reappears due to the competition between antiferromagnetic ( $(A, B)$ -symmetric) order, preferred in the  $H_p = 0$ -region, and a strongly ( $A, B$ )-asymmetric ferrimagnetic order for sufficiently large  $H_p/J$ .

We finally compare our 1RSB-results for the free energies in the double transition regime of Figs.3,4. Fig.5 provides evidence for the discontinuous transition to involve a transition from unmodulated to modulated *RSB*. As discussed in [1] higher energies correspond to improved solu-

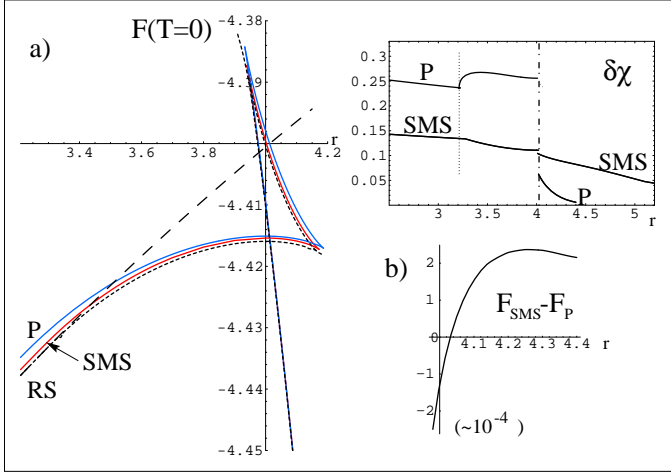


**Fig. 5.** a) Energies  $F(T=0)$  of modulated 1RSB- (arrow), unmodulated 1RSB- ( $P$ ), and RS-scheme ( $RS$ ) with ferromagnetic RS-solution (dashed), shown as a function of  $r \equiv J_{af}/J$  in the double transition region, b) energy difference between modulated- and unmodulated scheme; inset (top right) shows susceptibility RSB-contributions  $\delta\chi$ .

tions (unless identical stability criteria are met). Fig.5b) shows that the energy for the *SMS*-scheme is higher for  $J_{af} > J_{af}^c \approx 4.02$  (lower if  $<$  holds). This crossing of energies at the discontinuous transition and the character of the *RSB*-schemes suggests that modulated *RSB* governs the  $J_{af} > J_{af}^c$ -regime. The *RS*-solution is lowest but unstable everywhere. Despite small energy separation, equilibrium- and nonequilibrium linear susceptibility shows large differences which depend strongly on the type of *RSB*-scheme (inset of Fig.5). Further observable manifestations and thermal behavior remain to be considered.

## 5 Confined field-fraction effect on the multiplicity of phase transitions

The sublattice effective fields of Eq.6 help to explain the origin of the discontinuous transition: the competition between  $J_{af}M_{\bar{\kappa}}$  and the polaron field leads (in the clean limit) to a total spin reversal on one sublattice. Random magnetic order would smear the jump in any homogeneous field, as can be deduced from Fig.6 at  $\alpha = 1$ , but the discontinuity reappears due to the competition between antiferromagnetic ( $(A, B)$ -symmetric) order, preferred in the  $H_p = 0$ -region, and a strongly ( $A, B$ )-asymmetric ferrimagnetic order for sufficiently large  $H_p \neq 0$ . For half-penetrated layer ( $\alpha = 0.5$ ) the continuous transition with order parameter  $M_A - M_B$ , caused by the competition between spin glass and antiferromagnetic order, exists at  $J_{af} = J_{af}^c \approx 3.25J$ . To understand the  $\alpha = 0.5$ -scenario in the context of all  $0 \leq \alpha \leq 1$  we found sufficient to analyze the stability limits at  $T = 0$  in an *RS*-approximation. Introducing the definitions

$$\xi = r M_{\kappa}, h_p \equiv H_p/J \quad (10)$$

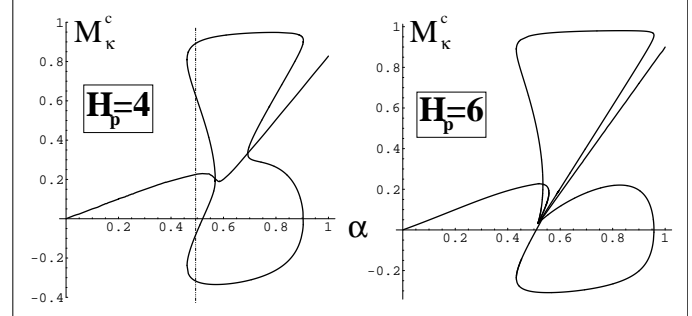


**Fig. 6.** Magnetizations  $M_{\kappa=A,B}^c$  obeying the constraint  $dM_{\kappa}^c/dr = \infty$ ,  $r \equiv J_{af}/J$ , are shown in *RS*-approximation for  $T = 0$  as a function of the polaron fraction  $\alpha$  for field strengths  $H_p = 4, 6$ ; the vertical line indicates the position of the double transition analyzed in 1RSB-schemes in Figs.3,4.

one may cast the equation of state into the compact nested form

$$\xi = u(u(\xi) + \eta u(\xi - h_p)) + \eta u(u(\xi) + \eta u(\xi - h_p) + h_p), \quad (11)$$

where

$$u(\xi) \equiv (1 - \alpha)r \operatorname{erf}(\xi/\sqrt{2}), \eta = \alpha/(1 - \alpha). \quad (12)$$

The stability limits are obtained under the constraint

$$\frac{dr(M_{\kappa})}{dM_{\kappa}} = 0, \frac{d^2r(M_{\kappa})}{dM_{\kappa}^2} \neq 0. \quad (13)$$

in terms of the inverted solution  $r(M_{\kappa})$  displaying the interaction ratio  $r \equiv J_{af}/J$  as a function of the sublattice magnetizations  $M_{\kappa}$ . The constrained solutions  $M_{\kappa}^c$  are derived by scanning all  $\alpha$  and shown in Fig.6 for typical values of  $H_p$  (stability limits in terms of  $J_{af}(\alpha)$  are omitted for brevity). At a fixed  $\alpha$ , the existence of one or three solutions implies a single continuous or a single discontinuous SG-ferrimagnetic transition respectively, while five solutions are necessary to obtain a double transition regime (with a magnetization-curve  $M(r = J_{af}/J)$  shaped as in Figs.3,4). Corrections in the effective field  $\tilde{H}$  originating from intra-sublattice interactions do not change qualitatively the results. The right part of Fig.6 shows a special point which emerges for large  $H_p$  near  $\alpha \approx 0.5$  and small  $M_{\kappa}^c$ .

The Korenblit-Shender model in a field  $h = H_p$  can be retrieved at  $\alpha = 1$ .

## 6 Conclusions and open ends

In this article hybrid *RSB*-schemes which combine tree- and wave-like structures were defined. A variational embedding factor of Parisi block matrices appeared as a characteristic ingredient of the new schemes. The application showed that the *SMS*-modulated phase is preferred beyond a critical  $J_{af}^c$  where a type of antiferromagnetic order prevails. The *MMS*-scheme (in contrast to *SMS*) allows

a continuous crossover to unmodulated *RSB* and should be analyzed as a candidate for glassy antiferromagnets. A generalization of our trace-formula to all powers of the order parameter matrix can create an extension of the Parisi scheme, modelling perhaps excited states in short-range spin glasses. Higher orders of both types of *RSB* are currently under study, using for example techniques applied to unmodulated *RSB* in Ref.[15].

## 7 Acknowledgements

We acknowledge support by the EPSRC (R.O. and D.S.), by the DFG, the SFB410 *II-VI semiconductors* (R.O. and M.K.), and by the ESF-programme SPHINX. We express our gratitude (R.O. and D.S.) for hospitality at MPI Heidelberg and for discussions with H.A. Weidenmüller.

## References

1. G. Parisi, Phys. Rev Lett. **50**, (1983) 1946
2. G. Parisi, J.Phys.A **13**, (1980) 1101
3. M. Palassini, A.P. Young, Phys.Rev.Lett.**85**, (2000) 3333
4. E. Marinari, G. Parisi, Phys.Rev.Lett.**85**, (2000) 3332
5. I.Ya. Korenblit, E.F. Shender, Sov.Phys.JETP**62**, (1985) 1030
6. D. Sherrington, S. Kirkpatrick, Phys. Rev. Lett. **35**, (1975) 1972
7. J.P. Bouchaud, M. Mézard, J. Physique **4**, (1994) 1109
8. E. Marinari, G. Parisi and F. Ritort, J. Phys A**27**, (1994) 7647
9. P. Chandra, L.B. Ioffe, D. Sherrington, Phys. Rev. Lett. **75**, (1995) 713
10. M. Mézard, G. Parisi, M.A. Virasoro, *Spin Glass Theory and Beyond* (World Scientific, Singapore, 1987)
11. J. Villain, Z.Phys.**B33**, (1979) 31
12. A.Chudnovskiy, R.Oppermann, B.Rosenow, D.Yakovlev, W.Zehnder, W.Ossau, Phys.Rev.**B55**, (1997) 10519
13. F. Bernardot, C.Rigaux, Phys.Rev.**B56**, (1997) 2328
14. C. Wengel, C.L. Henley, A. Zippelius, Phys.Rev.**B53**, (1995) 6543
15. R. Oppermann, D. Sherrington, Phys.Rev.**B67**, (2003) 245111